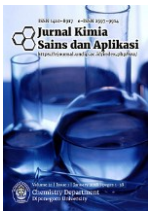
ISSN: 1410-8917
Jurnal Kimia Sains & Aplikasi
e-ISSN: 2597-9914

Jurnal Kimia Sains dan Aplikasi 29 (8) (2026): 545-553

Jurnal Kimia Sains dan Aplikasi
Journal of Scientific and Applied Chemistry

Journal homepage: http://ejournal.undip.ac.id/index.php/ksa



On-Off-On Fluorescent Potential Progesterone Detection Using N-Doped Carbon Dots from Oil Palm Empty Fruit Bunch

Elvina Dhiaul Iftitah [1,*], Diah Mardiana [1], Amalia Indah Anindia Darmawan [1], Aura Putri Farisca [1]

[1] Department of Chemistry, Faculty of Sciences, Technology, and Mathematics, Brawijaya University, Malang, Indonesia

* Corresponding author: vin_iftitah@ub.ac.id

https://doi.org/10.14710/jksa.29.8.545-553

Article Info

Article history:

Received: 12th June 2026
Revised: 19th September 2026
Accepted: 21st September 2026
Online: 30th September 2026

Keywords:
progesterone; carbon dots; oil palm empty fruit bunch; fluorescence biosensing; hydrogen peroxide

Abstract

Progesterone is an important steroid hormone involved in reproductive regulation and hormonal homeostasis, making its accurate determination essential for clinical and biomedical applications. In this study, nitrogen-doped carbon dots (N-CDs) were synthesized from oil palm empty fruit bunch (OPEFB) waste using o-phenylenediamine (o-PD) via a hydrothermal method and applied as a fluorescent biosensor for progesterone detection. Carbon dots (CDs) have attracted significant interest as fluorescent nanomaterials due to their excellent optical properties, stability, and biocompatibility. The synthesis condition of N- CDs was 180°C for 4 h, producing N-CDs with an average hydrodynamic size of 5.04 nm based on DLS analysis, while LR-TEM analysis showed individual N- CDs with an average size of 3.6 nm. The N-CDs exhibited good stability under pH 6–7. The sensing mechanism relied on a fluorescence on–off–on system involving N-CDs, H_2O_2, and progesterone, in which H_2O_2 quenched fluorescence via photoinduced electron transfer (PET), while progesterone restored the signal by inhibiting electron transfer. The developed sensor exhibited a linear response over the range of 20–100 nM, with an R^2 of 0.9956 and an LOD of 5.827 nM. Furthermore, the sensor exhibited recovery in fetal bovine serum (132.41% and 73.98%) with RSD values below 1%, demonstrating its potential as a simple and sensitive platform for progesterone detection in complex biological samples.

1. Introduction

Progesterone is an essential steroid hormone involved in reproductive regulation, pregnancy maintenance, and hormonal homeostasis [1, 2, 3, 4]. Abnormal progesterone levels have been associated with infertility, recurrent miscarriage, polycystic ovary syndrome, and hormone-related disorders, highlighting the importance of accurate progesterone monitoring in clinical and reproductive health applications [5, 6, 7, 8, 9, 10].

Various analytical techniques, including immunoassays and chromatographic methods, have been widely employed for the determination of progesterone [11, 12, 13, 14]. Although these established analytical tools deliver exceptional accuracy and low detection thresholds, their application is often limited by the need for sophisticated equipment, laborious sample preparation, and expensive specialized reagents. Moreover, highly selective approaches may depend on specific antibodies or enzymes, which can be relatively expensive, susceptible to stability issues, and require stringent storage conditions. Taken together, these limitations emphasize the need for analytical strategies that are simpler, faster, and more affordable. Carbon dot-based fluorescence sensing provides a potential approach to address this need through optical detection without the use of specific antibodies or enzymes [15].

Fluorescence sensing has become an attractive analytical alternative because it provides rapid analysis, high sensitivity, and straightforward experimental procedures [16]. Among fluorescent nanomaterials, carbon dots have attracted considerable attention because of their excellent photostability, low toxicity, high water solubility, and tunable surface chemistry [17,

18, 19, 20]. In addition, biomass-derived carbon dots offer a sustainable route for nanomaterial production by converting agricultural waste into value-added functional materials [21, 22]. Oil palm empty fruit bunch (OPEFB), generated in large quantities as a lignocellulosic residual stream from palm oil extraction facilities, serves as an exceptional carbonaceous matrix for CD synthesis due to its high concentration of polymer networks, including cellulose, hemicellulose, and lignin [23].

Nitrogen doping has been widely employed to improve the optical properties and sensing performance of carbon dots by enhancing electron density and introducing additional emissive surface states. Among various nitrogen precursors, o-phenylenediamine is particularly attractive because of its electron-rich amino groups and its ability to produce highly fluorescent nitrogen-doped carbon dots [16]. Furthermore, carbon dot-based progesterone sensing can be achieved via an on–off–on fluorescence-switching mechanism, in which fluorescence is initially quenched by a suitable quencher and subsequently restored upon interaction with the target analyte [16, 24].

In this study, we use H_2O_2 as a quencher. The quenching effect of H_2O_2 may involve oxidative interactions with the surface states of carbon dots, altering their electronic environment and promoting nonradiative deactivation of the excited state [16]. In addition, Jia et al. reported that H_2O_2-induced fluorescence quenching of carbon dots can be associated with a photoinduced electron transfer (PET) process, in which electron transfer from the excited emissive state to an electron acceptor leads to nonradiative deactivation [25]. Based on these reports, H_2O_2 was selected in the present study to establish the fluorescence "off" state before progesterone addition.

In contrast, metal ion quenchers generally interact with carbon dots through coordination with surface donor groups, such as amino, hydroxyl, and carboxyl groups. Although metal-ion-based systems can also produce fluorescence recovery through mechanisms such as competitive binding or displacement, this would introduce an additional metal-surface coordination process [26]. Therefore, the advantage of H_2O_2 in the present system is not claimed to be intrinsically higher selectivity, but its ability to provide a simple metal-free oxidative "off" state followed by a progesterone-induced "on" response. No specific chemical reaction or complex formation between progesterone and H_2O_2 is proposed, as this interaction was not directly investigated in the present study.

Although the H_2O_2-quenching/progesterone-recovery strategy has previously been reported using yellow-emissive carbon dots [16]. This study focuses on the use of OPEFB as a biomass-derived carbon precursor for synthesizing nitrogen-doped carbon dots (N-CDs) and their preliminary application to progesterone detection. The study therefore highlights the potential of OPEFB as a renewable carbon source for developing carbon-dot-based fluorescence-sensing materials via an on–off–on fluorescence-switching mechanism using hydrogen peroxide as the quencher.

2. Experimental

This study consisted of four main stages, namely the synthesis of N-CDs derived from OPEFB, physicochemical characterization of the synthesized materials, evaluation of fluorescence stability, and application of the N-CDs as a fluorescent biosensor for progesterone detection through an on-off-on fluorescence switching mechanism. The experimental procedures were designed to investigate the optical properties, structural characteristics, sensing performance, selectivity, and applicability of the developed sensing platform.

2.1. Equipment and Materials

The equipment used in this study included a 50 mL beaker glass, a 25 mL measuring cylinder, an analytical balance, an ultrasonic bath (Sonica), an oven (Memmert UNB 100), a 50 mL polytetrafluoroethylene-lined hydrothermal autoclave reactor, a 100 mL separatory funnel, a refrigerated centrifuge (Thermo Sorvall ST8R), a disposable syringe, a 0.22 µm nylon syringe filter, a petri dish, a freeze dryer, and 20-200 µL and 100-1000 µL micropipettes (SARANA).

The optical and structural characterizations were performed using a UV–visible spectrophotometer (Shimadzu UV-1601), fluorescence spectrometer (PerkinElmer LS 45), microplate reader (VANTAstar BMG LABTECH), ATR-FTIR (Shimadzu IR-Spirit), dynamic light scattering (DLS; BIOBASE), and low-resolution transmission electron microscopy (LR-TEM) (JEM-2100Plus JEOL).

The materials used in this work were oil palm empty fruit bunch obtained from PT Polytech Indonesia, o- phenylenediamine (o-PD; ≥99%, Merck), ultrapure water (Ikapharmindo), dichloromethane (≥99.8%, SmartLab), progesterone (≥98%, Sigma Aldrich), rhodamine B (≥95%, Sigma Aldrich), ethanol (analytical grade, SmartLab), hydrogen peroxide (30%, SmartLab), glycine (≥99%, Merck), glucose (≥99.5%, Merck), citric acid (≥99.5%, Merck), ascorbic acid (≥99%, Merck), Tween 80 (analytical grade, SmartLab), Britton–Robinson buffer solution (boric acid, citric acid, and $Na_3PO_4.10H_2O$), phosphate-buffered saline (PBS; Merck), and fetal bovine serum (FBS; HyClone™ Characterized FBS, US Origin, Cytiva; catalog no. SH30071.02; Lot/Serial No. AJ30726118(1)).

The manufacturer's specifications for FBS include endotoxin ≤25 EU/mL and hemoglobin <25 mg/dL, with no bacterial or fungal growth detected in sterility testing. The serum was also tested for specified viral contaminants, cytopathogenic and hemadsorbing agents, and mycoplasma, all of which were reported as not detected. In addition, the progesterone concentration in the FBS was experimentally determined using a chemiluminescent immunoassay (CLIA) at Rampal Diagnostika Clinical Laboratory and was found to be <0.05 ng/mL.

2.2. Experimental Procedures

2.2.1. Synthesis of N-CDs

The OPEFB was first chopped using a chopper and then sieved until a sufficiently fine powder was obtained. The resulting powder was stored in a closed container until further use. The preparation of N-CDs commenced by combining 50 mg of finely pulverized OPEFB with 250 mg of o-PD. This solid mixture was then suspended in a 20 mL volume of ultrapure water. To guarantee a completely uniform and homogeneous particle dispersion, the liquid mixture was subjected to ultrasonic processing for 15 minutes. Following sonication, the blended precursor was transferred into a 50 mL Teflon-lined stainless steel autoclave system. Hydrothermal carbonization was subsequently performed by placing the sealed vessel in a laboratory oven maintained at 180°C for 4 hours. After the reaction was completed and the system was allowed to cool naturally to room temperature, the resulting product was purified by liquid–liquid extraction using 20 mL of dichloromethane and 20 mL of the aqueous phase, corresponding to a 1:1 volume ratio. The aqueous fraction containing the N-CDs was collected, followed by centrifugation at 8000 rpm for 30 min, filtration through a 0.22 µm nylon membrane, and freeze-drying to obtain N-CDs powder.

The optical characteristics of the obtained N-CDs were evaluated using ultraviolet–visible and fluorescence spectroscopy. For UV–Vis analysis, the N-CDs solution obtained before freeze-drying was diluted 400-fold with distilled water for measurement. The excitation and emission fluorescence profiles were measured using a PerkinElmer LS 45 spectrofluorometer at an N-CDs concentration of 0.01 mg/mL, with both excitation and emission slit widths set to 10 nm. Quantum yield measurements were performed using rhodamine B in water as the reference standard, with a reported quantum yield of 0.36 [27]. The N-CDs sample and rhodamine B reference were prepared in water and measured at an excitation wavelength of 420 nm. The quantum yield (QY) was calculated using the slope method by plotting the integrated fluorescence intensity against the absorbance at different concentrations. The QY was calculated from the ratio of the slopes obtained for the N-CDs and rhodamine B, with correction for the refractive index of the respective solvents.

2.2.2. Characterization of N-CDs

Functional groups were characterized by ATR-FTIR spectroscopy, whereas DLS diagnostics provided data regarding hydrodynamic size distributions and LR-TEM for size measurement. The measurement conditions for the characterization techniques were as follows. For ATR-FTIR analysis, the freeze-dried N-CDs powder was placed directly onto the ATR crystal, and the spectra were recorded over the wavenumber range of 400–4000 cm^{-1}. The obtained spectra were compared with those of the corresponding precursors. For DLS analysis, the freeze-dried N-CDs powder was dispersed in distilled water at a concentration of 0.1 mg/mL and sonicated for 15 minutes before measurement. TEM analysis was performed using the N-CDs sample prepared by the UNDIP laboratory.

2.2.3. pH-Dependent Fluorescence Response of N-CDs

Environmental endurance trials for carbon dots were also undertaken. Specifically, the optical resilience under shifting acidity profiles was mapped by tracking the N-CDs responses inside Britton-Robinson buffer configurations spanning a pH gradient from 4.0 to 12.0. The Britton–Robinson buffer was prepared using 0.2 M boric acid, 0.05 M citric acid, and 0.1 M $Na_3PO_4{\cdot}10H_2O$, with the components mixed at the volume ratios reported in the literature [28]. The pH response was evaluated by mixing 1 mL of N-CDs at a concentration of 0.4 mg/mL with 1 mL of Britton–Robinson buffer at each pH from 4 to 12, yielding a sample-to-buffer volume ratio of 1:1.

2.2.4. Progesterone Sensing Using N-CDs

For progesterone sensing, fluorescence quenching was first induced by adding hydrogen peroxide (30%) to the N-CDs solution. A progesterone stock solution was prepared in ethanol containing Tween 80 and diluted to obtain working solutions. Various progesterone concentrations (0–100 nM) were added to the quenched N-CDs system, and fluorescence recovery was measured using a fluorescence spectrometer. The sensing performance was evaluated based on the relationship between fluorescence intensity and progesterone concentration.

To investigate the effect of H_2O_2 on the fluorescence of the N-CDs, 200 µL of N-CDs solution (0.2 mg/mL) was mixed with 500 µL of H_2O_2 solution and 500 µL of progesterone solvent containing ethanol, ultrapure water, and Tween 80, but without progesterone. Ultrapure water was added to obtain a total reaction volume of 2 mL. The H_2O_2 solution was prepared as a fourfold concentrated solution, and the amount of H_2O_2 was varied to obtain final H_2O_2 volumes of 0, 20, 40, 60, 80, 100, and 120 µL, corresponding to nominal final concentrations of 0, 0.3, 0.6, 0.9, 1.2, 1.5, and 1.8%, respectively, based on the 30% H_2O_2 stock solution. The progesterone solvent contained ethanol, ultrapure water, and Tween 80 at final concentrations of approximately 77.56% ethanol and 0.022% Tween 80. The mixtures were incubated for 10 min at room temperature before fluorescence measurement.

For progesterone sensing, the optimized H_2O_2 condition was subsequently applied. The progesterone stock solutions were prepared at fourfold the desired final concentrations to compensate for the fourfold dilution upon addition to the 2 mL reaction mixture. Progesterone concentrations were varied to obtain final concentrations of 0–100 nM. The reaction mixture consisted of 200 µL of N-CDs solution (0.2 mg/mL), 500 µL of the optimized H_2O_2 solution (1.8%), 500 µL of progesterone solution, and 800 µL of ultrapure water, giving a total volume of 2 mL and a final N-CDs concentration of 0.02 mg/mL. The progesterone solution was prepared using ethanol, ultrapure water, and Tween 80. The mixture was incubated for 10 minutes at room temperature before fluorescence measurement. Fluorescence spectra were recorded using a PerkinElmer LS45 fluorescence spectrometer at an excitation wavelength of 420 nm, with slit widths of 10 nm.

2.2.5. Selectivity and Application in Biological Samples

Selectivity experiments were performed using glycine, glucose, citric acid, and ascorbic acid as potential interfering compounds at identical concentrations. Finally, the applicability of the developed sensing platform was investigated using progesterone-spiked FBS samples. Prior to progesterone spiking, the FBS samples were diluted with PBS at a dilution factor of 40. Progesterone was then added to the diluted FBS samples at the desired concentrations. The fluorescence response was recorded after incubation, and the recovery percentage was calculated to evaluate analytical performance in a biological matrix.

The selectivity of the proposed fluorescence sensing system was evaluated using the same procedure as the progesterone sensing experiment. Briefly, 200 µL of N-CDs solution (0.2 mg/mL), 500 µL of the H_2O_2 1.8%, 500 µL of the test solution (100 nM final concentration), and 800 µL of ultrapure water were mixed to obtain a total reaction volume of 2 mL. For the interference study, progesterone was replaced individually with glycine, glucose, citric acid, or ascorbic acid. For the FBS test, progesterone was replaced with FBS. The mixtures were incubated for 10 min at room temperature before fluorescence measurement. All measurements were performed using a PerkinElmer LS 45 fluorescence spectrometer at an excitation wavelength of 420 nm, with both excitation and emission slit widths set to 10 nm.

3. Results and Discussion

3.1. Optical Properties of N-CDs

The optical properties of the synthesized N-CDs were investigated to evaluate their absorption and fluorescence characteristics. UV–Vis absorption spectroscopy was used to identify the characteristic absorption features of the N-CDs, while fluorescence spectroscopy was employed to examine their emission behavior. In addition, the fluorescence QY was determined to assess the efficiency of their fluorescence emission. Spectrophotometric analysis of the prepared N-CDs revealed a dual-peak profile located near 259 nm and 420 nm, as shown in Figure 1. The shorter wavelength peak in the ultraviolet band signifies the characteristic $\pi-\pi^*$ electronic transition within the localized sp^2 networks of the carbonaceous core. Concurrently, the wider profile appearing in the visible spectrum indicates the presence of $n-\pi^*$ transitions, which are directly connected to the nitrogenous functional networks anchored on the outer edges of the dots [29].

As shown in Figure 2, the N-CDs exhibit a maximum excitation at 420 nm and a strong fluorescence emission at 560 nm, indicating yellow–orange fluorescence. Furthermore, the visual appearance of the synthesized N-CDs under visible light and UV irradiation is shown in Figure 3. The N-CDs appear as a clear solution under normal light and exhibit yellow-orange fluorescence under UV irradiation, confirming fluorescence emission and supporting their further investigation for fluorescence-based sensing applications.

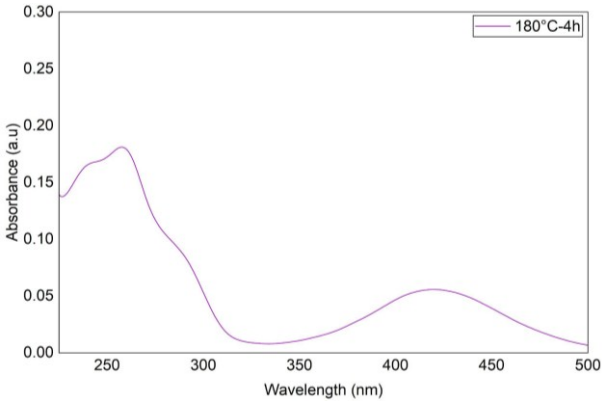


Figure 1. UV–Vis spectrum of N-CDs

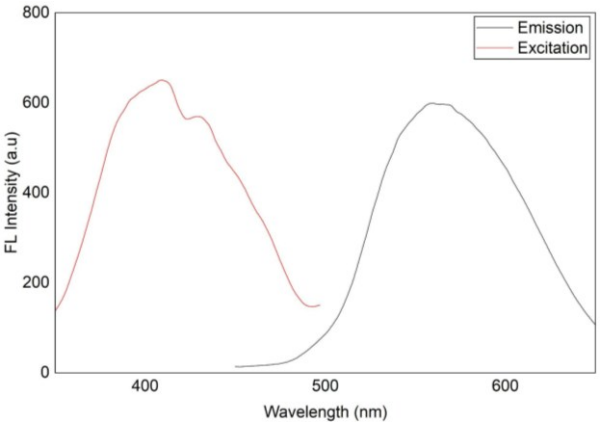


Figure 2. Excitation and emission spectra of N-CDs

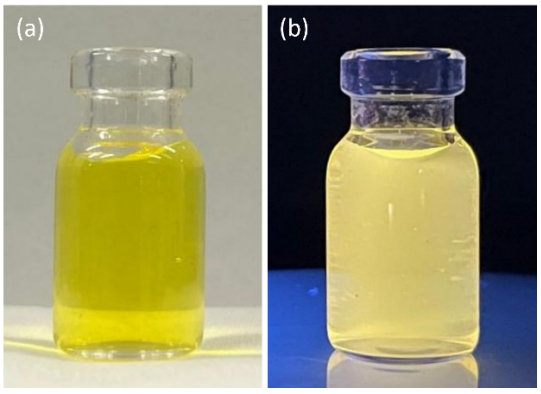


Figure 3. N-CDs (a) Daylight (b) Under UV light

The QY of the N-CDs was determined to be 2.16%. This value is relatively low compared with those commonly reported for carbon dots. However, a low QY does not necessarily limit the application of CDs as fluorescent sensing materials. A previous study reported carbon dots with a QY of 2.31% that were still capable of detecting Cr(VI) ions with a detection limit of 8 ppm [30]. Therefore, despite their relatively low QY, the CDs synthesized in this study still show potential for further development as fluorescent sensing materials.

3.2. Characterization of N-CDs

The FTIR spectrum in Figure 4 revealed the presence of hydroxyl, amino, carbonyl, aromatic carbon, and carbon–nitrogen functional groups on the N-CD surface. The broad absorption band observed around 3200–3400 cm^{-1} corresponded to O–H and N–H stretching

vibrations, whereas the absorption regions between 1628 and 1595 cm^{-1} were assigned to C=O, C=N, and aromatic C=C groups. Absorption at 1270 cm^{-1} corresponded to C- N. These results provide qualitative evidence of nitrogen-containing functional groups on the N-CD surface, which may originate from o-PD used during synthesis. However, FTIR alone does not quantitatively confirm nitrogen incorporation or its bonding states within the carbon framework. For more accurate confirmation of nitrogen incorporation and its bonding states, further analysis using X-ray photoelectron spectroscopy (XPS) would be recommended [31].

DLS analysis showed an average particle size of 5.04 nm with a PDI of 0.18 (Figure 5a). Since carbon dots are generally reported to have particle sizes below 10 nm, the obtained results support the presence of relatively small and dispersed N-CDs with a narrow hydrodynamic size distribution and relatively homogeneous particle sizes [32]. To further confirm the particle size and morphology, TEM analysis was performed using LR-TEM, which revealed an average particle diameter of 3.6 nm (Figure 5b-c). The slightly smaller size observed by TEM compared with DLS can be attributed to differences in measurement principles: DLS measures the hydrodynamic diameter of particles in dispersion, whereas TEM directly visualizes the particle core.

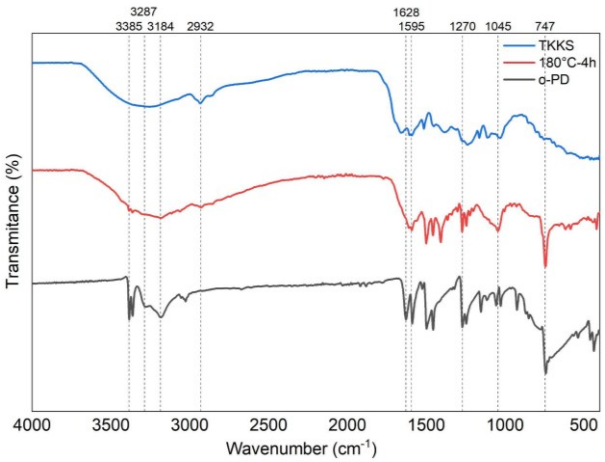


Figure 4. FTIR spectra of N-CDs

3.3. pH-Dependent Fluorescence Response of N-CDs

The FL intensity of N-CDs, as shown in Figure 6, was strongly influenced by the pH of the surrounding environment due to protonation and deprotonation of surface functional groups. Under acidic conditions, amino groups on the N-CDs surface may become protonated to $-NH_3^+$, altering the surface electronic states and increasing non-radiative relaxation pathways, thereby reducing fluorescence intensity. The maximum fluorescence intensity was observed at neutral pH, where the surface functional groups remained relatively stable, thereby allowing efficient electron–hole recombination. At higher pH, deprotonation of surface groups modified the surface charge distribution and disturbed the electronic environment, leading to a reduction in fluorescence intensity [33]. Although the fluorescence intensity varied under different pH conditions, the N-CDs retained substantial fluorescence at pH 7, which is close to the physiological blood pH range of 7.35–7.45 [34]. Although pH 7 does not represent the entire physiological range, this result provides an initial indication that the N- CDs may be suitable for further investigation under near-physiological conditions.

3.4. Potential Fluorescence Sensing Performance toward Progesterone

3.4.1. Fluorescence Quenching of N-CDs by H_2O_2

The fluorescence on–off–on sensing platform was established using H_2O_2 as a quencher. Upon the addition of H_2O_2, the fluorescence intensity of N-CDs gradually decreased without a noticeable shift in the emission maximum, as shown in Figure 7. The absence of spectral shifts indicates that H_2O_2 did not generate new emissive centers but reduced the fluorescence efficiency of the existing N-CDs surface states. The quenching process is attributed to a PET mechanism, in which H_2O_2 acts as an electron acceptor, facilitating electron transfer from the excited N-CDs and thereby promoting non-radiative relaxation pathways. In addition, oxidation of surface fluorophores by H_2O_2 may create additional defect states that further accelerate fluorescence quenching [25].

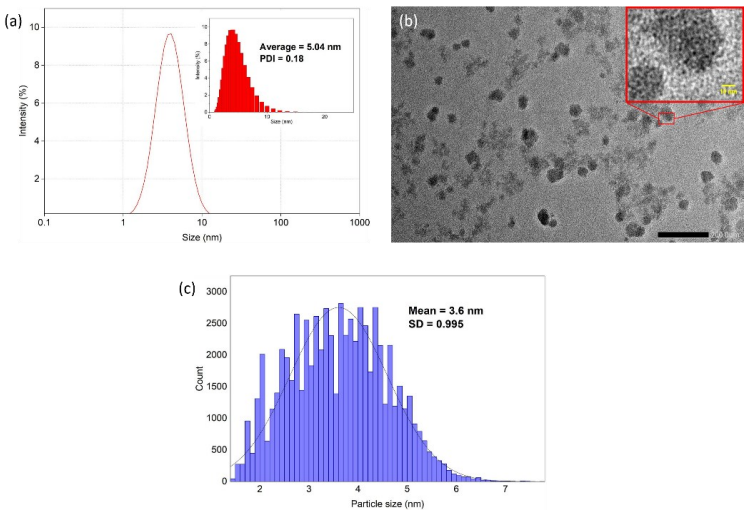


Figure 5. (a) Size distribution of N-CDs using DLS, (b) LR-TEM image, and (c) Size distribution of N-CDs using LR- TEM

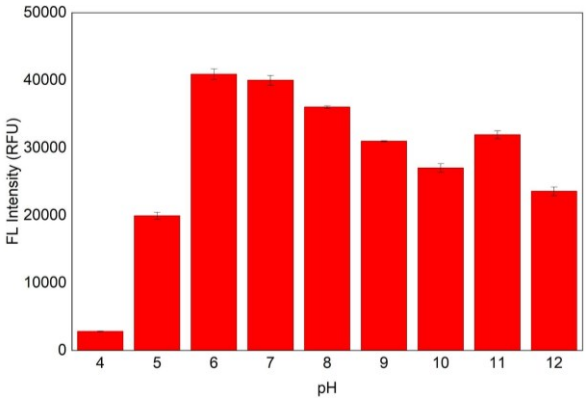


Figure 6. pH-dependent fluorescence response of N-CDs

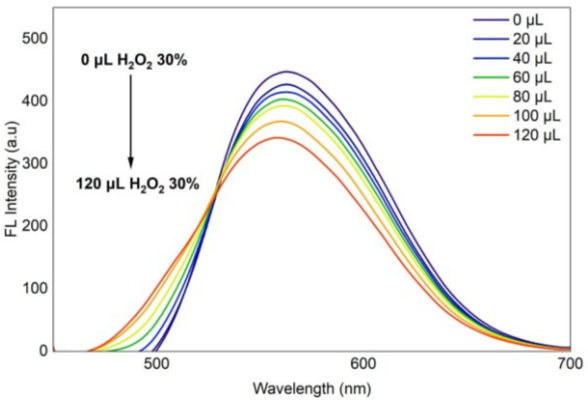


Figure 7. Fluorescence quenching curve of N-CDs by H_2O_2

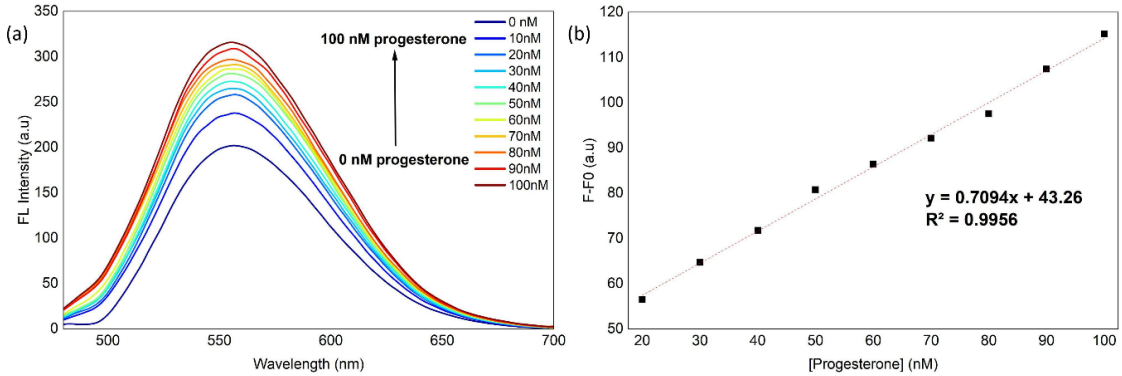


Figure 8. (a) Fluorescence intensity of N-CDs–H_2O_2 after the addition of progesterone (0–100 nM) and (b) Calibration curve of F–F_0 versus progesterone concentration (20–100 nM)

3.4.2. Detection of Progesterone

Following the establishment of the fluorescence "off" state using H_2O_2, the potential of the N-CDs for progesterone detection was further investigated by monitoring the fluorescence recovery upon progesterone addition. Figure 8 shows the fluorescence response of N-CDs toward different progesterone concentrations. After the formation of the quenched N-CDs–H_2O_2 system, the addition of progesterone resulted in gradual fluorescence recovery. The fluorescence intensity increased with increasing progesterone concentration from 0 to 100 nM without altering the emission profile, indicating that progesterone did not generate a new fluorescent species but restored the original emissive process of N-CDs.

Previous studies have proposed that progesterone may restore fluorescence by reducing oxidized surface groups on N-CDs. However, this mechanism remains speculative because direct evidence from XPS is still limited [16]. Therefore, the fluorescence recovery in this study is more reasonably explained by the suppression of PET between the N-CDs surface and H_2O_2, allowing excited electrons to return to the ground state through radiative pathways, resulting in increased fluorescence emission [25]. This interpretation is tentative and is based on the observed fluorescence response and previously reported behavior of carbon dots. Further studies, such as time-resolved fluorescence or electrochemical measurements, are needed to directly verify the proposed PET process.

An exceptionally linear correlation spanning from 20 to 100 nM was established between the differential photoluminescence intensity (F–F_0) and the actual concentration of progesterone. This analytical relationship is defined by the mathematical expression y = 0.7094x + 43.26, yielding an outstanding coefficient of determination (R^2) of 0.9956. Furthermore, the fabricated biosensing architecture exhibits substantial diagnostic sensitivity, as evidenced by a low limit of detection (LOD) of 5.827 nM and a limit of quantification (LOQ) of 19.424 nM. The LOD and linear detection range of the proposed method, compared with previously reported materials, are summarized in Table 1.

Table 1. Comparison of LOD and linear detection range of progesterone using various materials

Material	Detection method	LOD (nM)	Linear range	Year	Ref.
QDs hydrogel	Fluorescence	55	78–632 nM	2020	[35]
CDs	Fluorescence	10.25	0–200 µM	2020	[16]
CDs-GO	Photoelectrochemical	0.17	0.5–180 nM	2020	[36]
CDs	Fluorescence	9.3	0–130 µM	2021	[37]
CDs	Fluorescence	13.8	10–900 nM	2022	[38]
N-CDs	Fluorescence	5.827	20–100 nM	2026	This work

3.4.3. Selectivity Test

As shown in Figure 9, the selectivity study demonstrated that progesterone induced a significantly greater fluorescence recovery than other interfering compounds, including glycine, glucose, citric acid, and ascorbic acid. This result indicates the favorable interaction between progesterone and the surface states of N-CDs, which may be influenced by differences in molecular structure, polarity, and functional groups. In contrast, the relatively weak responses of the interfering molecules suggest their limited interaction with the N- CDs-based sensing system. However, the detailed interaction mechanism responsible for the selective fluorescence recovery of progesterone requires further investigation using advanced surface characterization and mechanistic studies.

3.4.4. Application in Real Sample (Fetal Bovine Serum)

To evaluate the applicability of the proposed method in a biological matrix, progesterone recovery experiments were performed using FBS samples. Known concentrations of progesterone were spiked into FBS, and the fluorescence response was measured using the proposed N-CD-based method. The recovery and precision results are summarized in Table 2. Recovery values of 132.41% and 73.98% were obtained for 50 and 100 nM progesterone, respectively, indicating possible signal enhancement and suppression by matrix components such as proteins and other biomolecules. Similar variations in recovery have been reported for N- CD-based sensors applied to serum samples, with recovery values ranging from 86.32% to 97.53% [39]. The low RSD values (<1%) indicate excellent repeatability, suggesting that the recovery deviation was mainly influenced by matrix effects rather than poor analytical precision.

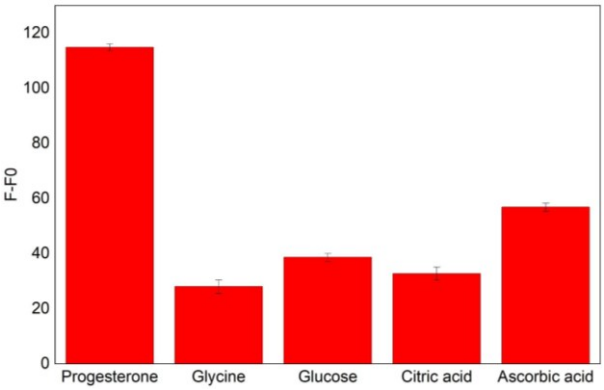


Figure 9. Selectivity study of the N-CDs-H_2O_2 fluorescence system toward progesterone and other interfering compounds

Table 2. Comparison of progesterone spike recovery in FBS samples

Sample	[Progesterone] added (nM)	[Progesterone] detected (nM)	Recovery (%)	RSD (%; n=3)
FBS	50	66.2	132.41	0.284
FBS	100	73.98	73.98	0.304

4. Conclusion

Carbon dots derived from OPEFB were successfully synthesized through a hydrothermal method and exhibited favorable optical properties. The developed N- CDs-H_2O_2 fluorescence on-off-on sensing system showed a sensitive response toward progesterone with a linear range of 20–100 nM and a low detection limit of 5.827 nM. Moreover, the sensor demonstrated good selectivity and acceptable performance in fetal bovine serum samples, indicating its potential as a simple and promising fluorescent platform for progesterone detection in complex biological matrices.

Acknowledgment

The authors gratefully acknowledge the Integrated Research Laboratory, Brawijaya University, for its cooperation in providing access to instrumentation. The authors also acknowledge financial support from the Brawijaya University Internal Research Grant Scheme B.

References

[1] Sarmila Mustakim, Nasrudin Andi Mappaware, Arni Isnaini Arfah, Hamzah Said, Zulfamidah Zulfamidah, Pengaruh Buah Kurma Ajwa (*Phoenix dactylifera* L) Terhadap Kadar Hormon Progesteron, *Innovative: Journal of Social Science Research*, 4, 1, (2024), 4862-4871

[2] M. Schumacher, R. Hussain, N. Gago, J. P. Oudinet, C. Mattern, A. M. Ghoumari, Progesterone Synthesis in the Nervous System: Implications for Myelination and Myelin Repair, *Frontiers in Neuroscience*, 6, (2012), 10 https://doi.org/10.3389/fnins.2012.00010

[3] R. C. Melcangi, S. Giatti, D. Calabrese, M. Pesaresi, G. Cermenati, N. Mitro, B. Viviani, L. M. Garcia-Segura, D. Caruso, Levels and actions of progesterone and its metabolites in the nervous system during physiological and pathological conditions, *Progress in Neurobiology*, 113, (2014), 56-69 https://doi.org/10.1016/j.pneurobio.2013.07.006

[4] J. A. MacLean, K. Hayashi, Progesterone Actions and Resistance in Gynecological Disorders, *Cells*, 11, 4, (2022), 647 https://doi.org/10.3390/cells11040647

[5] B. Nagy, J. Szekeres-Barthó, G. L. Kovács, E. Sulyok, B. Farkas, Á Várnagy, V. Vértes, K. Kovács, J. Bódis, Key to Life: Physiological Role and Clinical Implications of Progesterone, *International Journal of Molecular Sciences*, 22, 20, (2021), 11039 https://doi.org/10.3390/ijms222011039

[6] N. Ranisavljevic, S. Huberlant, M. Montagut, P. M. Alonzo, B. M. Darné, S. Languille, T. Anahory, I. Cedrin-Durnerin, Low Luteal Serum Progesterone Levels are Associated with Lower Ongoing Pregnancy and Live Birth Rates in Art: Systematic Review and Meta-Analyses, *Fertility and Sterility*, 114, 3, (2020), E334-E335 https://doi.org/10.1016/j.fertnstert.2020.08.904

[7] A. J. Devall, A. Papadopoulou, M. Podesek, D. M. Haas, M. J. Price, A. Coomarasamy, I. D. Gallos, Progestogens for preventing miscarriage: A network meta-analysis, *Cochrane Database of Systematic Reviews*, 2021, 4, (2021), CD013792 https://doi.org/10.1002/14651858.CD013792.pub2

[8] Beena Darjee, Srijana Sharma, Sarita Rai, Biswash Chettri, Yugraj Chettri, Shelly H. Tuccu, Anupama

Moirangthem, Ayan Chatterjee, Impact of Hormonal Imbalance during Menstrual Cycle: A Review, *Clinical Research and Studies*, 4, 2, (2025), https://doi.org/10.31579/2835-2882/082

[9] M. Bataa, E. Abdelmessih, F. Hanna, Exploring Progesterone Deficiency in First-Trimester Miscarriage and the Impact of Hormone Therapy on Foetal Development: A Scoping Review, *Children*, 11, 4, (2024), 422 https://doi.org/10.3390/children11040422

[10] T. J. Lai, S. W. Teng, C. K. Chang, C. Y. Huang, Progesterone in Pregnancy: Evidence-Based Strategies to Reduce Miscarriage and Enhance Assisted Reproductive Technology, *Medical Science Monitor*, 30, (2024), e943400 https://doi.org/10.12659/MSM.943400

[11] W. Sun, Q. Xu, J. Sun, X. Lin, H. Pan, Design and Development of Biosensors for Progesterone Detection, *Journal of Sensors*, 2023, (2023), 4803143 https://doi.org/10.1155/2023/4803143

[12] A. Sangjan, S. Boonsith, K. Sansanaphongpricha, T. Thinbanmai, S. Ratchahat, N. Laosiripojana, K. C. W. Wu, H. S. Shin, C. Sakdaronnarong, Facile preparation of aqueous-soluble fluorescent polyethylene glycol functionalized carbon dots from palm waste by one-pot hydrothermal carbonization for colon cancer nanotheranostics, *Scientific Reports*, 12, (2022), 10550 https://doi.org/10.1038/s41598-022-14704-x

[13] Y. Wang, T. Zhang, H. Zhao, W. Zhou, J. Zeng, J. Zhang, C. Zhang, W. Chen, Measurement of serum progesterone by isotope dilution liquid chromatography tandem mass spectrometry: A candidate reference method and its application to evaluating immunoassays, *Analytical and Bioanalytical Chemistry*, 411, 11, (2019), 2363-2371 https://doi.org/10.1007/s00216-019-01676-7

[14] M. Z. Nouri, K. J. Kroll, M. Webb, N. D. Denslow, Quantification of steroid hormones in low volume plasma and tissue homogenates of fish using LC-MS/MS, *General and Comparative Endocrinology*, 296, (2020), 113543 https://doi.org/10.1016/j.ygcen.2020.113543

[15] H. Lee, C. J. Park, G. Lee, Measurement of progesterone in human serum by isotope dilution liquid chromatography–tandem mass spectrometry and comparison with the commercial chemiluminescence immunoassay, *Analytical and Bioanalytical Chemistry*, 396, (2010), 1713-1719 https://doi.org/10.1007/s00216-009-3410-8

[16] L. Cao, L. Yu, J. Yue, Y. Zhang, M. Ge, L. Li, R. Yang, Yellow-emissive carbon dots for "off-and-on" fluorescent detection of progesterone, *Materials Letters*, 271, (2020), 127760 https://doi.org/10.1016/j.matlet.2020.127760

[17] T. Sarkar, H. B. Bohidar, P. R. Solanki, Carbon dots-modified chitosan based electrochemical biosensing platform for detection of vitamin D, *International Journal of Biological Macromolecules*, 109, (2018), 687-697 https://doi.org/10.1016/j.ijbiomac.2017.12.122

[18] K. Ghosal, A. Ghosh, Carbon dots: The next generation platform for biomedical applications, *Materials Science and Engineering: C*, 96, (2019), 887-903 https://doi.org/10.1016/j.msec.2018.11.060

[19] S. Sen, A. Bose, Carbon dots: A review of innovations, applications, challenges, and future prospects, *Inorganic Chemistry Communications*, 173, (2025), 113852 https://doi.org/10.1016/j.inoche.2024.113852

[20] M. Jorns, D. Pappas, A Review of Fluorescent Carbon Dots, Their Synthesis, Physical and Chemical Characteristics, and Applications, *Nanomaterials*, 11, 6, (2021), 1448 https://doi.org/10.3390/nano11061448

[21] C. Kang, Y. Huang, H. Yang, X. F. Yan, Z. P. Chen, A Review of Carbon Dots Produced from Biomass Wastes, *Nanomaterials*, 10, 11, (2020), 2316 https://doi.org/10.3390/nano10112316

[22] H. P. Pham, K. K. Nguyen, T. T. Huynh, T. K. H. Pham, H. D. Ngo, Synthesis and characterization of carbon dots derived from biomass sources, *Dong Thap University Journal of Science*, 14, 5, (2024), 20-25 https://doi.org/10.52714/dthu.14.5.2025.1402

[23] F. Anindita, L. Naani, D. Permana, K. Karelius, Y. I. Kedang, Study on Utilizing Oil Palm Empty Fruit Bunch Waste into Carbon Nanodots, *Journal of The Indonesian Society of Integrated Chemistry*, 16, 2, (2024), 140-146 10.22437/jisic.v16i2.38583

[24] J. Tian, M. An, X. Zhao, Y. Wang, M. Hasan, Advances in Fluorescent Sensing Carbon Dots: An Account of Food Analysis, *ACS Omega*, 8, 10, (2023), 9031-9039 https://doi.org/10.1021/acsomega.2c07986

[25] J. Jia, X. Liu, W. Wang, Nitrogen-Doped Carbon Dots as a Fluorescent "Off–On" Probe for Selective Ascorbic Acid Detection via H_2O_2-Mediated Quenching, *Nanomaterials*, 15, 13, (2025), 976 https://doi.org/10.3390/nano15130976

[26] Z. L. Chen, R. Z. Xiao, J. C. Jin, L. Zeng, S. J. Sun, J. Q. Xu, Affinity-mediated photoluminescence quenching between metallic ions and surface functional groups of carbon nanodots, *Colloids and Surfaces A: Physicochemical and Engineering Aspects*, 634, (2022), 127940 https://doi.org/10.1016/j.colsurfa.2021.127940

[27] X. F. Zhang, Y. Zhang, L. Liu, Fluorescence lifetimes and quantum yields of ten rhodamine derivatives: Structural effect on emission mechanism in different solvents, *Journal of Luminescence*, 145, (2014), 448-453 https://doi.org/10.1016/j.jlumin.2013.07.066

[28] K. Ganesh, R. Soumen, Y. Ravichandran, Janarthanan, Dynamic approach to predict pH profiles of biologically relevant buffers, *Biochemistry and Biophysics Reports*, 9, (2017), 121-127 https://doi.org/10.1016/j.bbrep.2016.11.017

[29] H. O. Faleke, D. Pappas, *In vitro* detection of iron overload in leukemia cells using o-phenylenediamine-derived carbon dots, *Next Materials*, 8, (2025), 100667 https://doi.org/10.1016/j.nxmate.2025.100667

[30] K. Anpalagan, H. Yin, I. Cole, T. Zhang, D. T. H. Lai, Quantum Yield Enhancement of Carbon Quantum Dots Using Chemical-Free Precursors for Sensing Cr (VI) Ions, *Inorganics*, 12, 4, (2024), 96 https://doi.org/10.3390/inorganics12040096

[31] K. Nandhini, M. Ilanchelian, Nitrogen-Doped Carbon Dots with Aggregation-Induced Emission Enhancement for Selective Biosensing of Spermine,

Journal of Fluorescence, 35, (2025), 11261-11271 https://doi.org/10.1007/s10895-025-04373-0

[32] X. Li, L. Yan, J. Si, H. Xu, Y. Xu, Tuning the photoluminescence property of carbon dots by ultraviolet light irradiation, *RSC Advances*, 9, 22, (2019), 12732-12736 https://doi.org/10.1039/C9RA02080B

[33] W. K. Szapoczka, A. L. Truskewycz, T. Skodvin, B. Holst, P. J. Thomas, Fluorescence intensity and fluorescence lifetime measurements of various carbon dots as a function of pH, *Scientific Reports*, 13, (2023), 10660 https://doi.org/10.1038/s41598-023-37578-z

[34] H. Ozdemir, M. I. Sasmaz, R. Guven, A. Avci, Interpretation of acid–base metabolism on arterial blood gas samples via machine learning algorithms, *Irish Journal of Medical Science (1971 -)*, 194, (2025), 277-287 https://doi.org/10.1007/s11845-024-03767-6

[35] Mingfu Chen, Chloé Grazon, Prerana Sensharma, Thuy T. Nguyen, Yunpeng Feng, Margaret Chern, R. C. Baer, Nitinun Varongchayakul, Katherine Cook, Sébastien Lecommandoux, Catherine M. Klapperich, James E. Galagan, Allison M. Dennis, Mark W. Grinstaff, Hydrogel-Embedded Quantum Dot–Transcription Factor Sensors for Quantitative Progesterone Detection, *ACS Applied Materials & Interfaces*, 12, 39, (2020), 43513-43521 https://doi.org/10.1021/acsami.0c13489

[36] Y. Zhu, Z. Xu, J. Gao, W. Ji, J. Zhang, An antibody-aptamer sandwich cathodic photoelectrochemical biosensor for the detection of progesterone, *Biosensors and Bioelectronics*, 160, (2020), 112210 https://doi.org/10.1016/j.bios.2020.112210

[37] M. Zan, S. An, L. Cao, Y. Liu, L. Li, M. Ge, P. Liu, Z. Wu, W. F. Dong, Q. Mei, One-pot facile synthesis of yellow-green emission carbon dots for rapid and efficient determination of progesterone, *Applied Surface Science*, 566, (2021), 150686 https://doi.org/10.1016/j.apsusc.2021.150686

[38] Disha, P. Kumari, M. K. Patel, P. Kumar, M. K. Nayak, Carbon Dots Conjugated Antibody as an Effective FRET-Based Biosensor for Progesterone Hormone Screening, *Biosensors*, 12, 11, (2022), 993 https://doi.org/10.3390/bios12110993

[39] Arash Mohammadinejad, Khalil Abnous, Morteza Alinezhad Nameghi, Roghayeh Yahyazadeh, Sara Hamrah, Fereshteh Senobari, Seyed Ahmad Mohajeri, Application of green-synthesized carbon dots for imaging of cancerous cell lines and detection of anthraquinone drugs using silica-coated CdTe quantum dots-based ratiometric fluorescence sensor, *Spectrochimica Acta Part A: Molecular and Biomolecular Spectroscopy*, 288, (2023), 122200 https://doi.org/10.1016/j.saa.2022.122200